# Improved Error Protection for Uplink Control Signaling in 3GPP-LTE via Complex-Field Coding

Chaitanya Tumula V. K., Erik G. Larsson and Niclas Wiberg



Chaitanya Tumula V. K., Erik G. Larsson and Niclas Wiberg, Improved Error Protection for Uplink Control Signaling in 3GPP-LTE via Complex-Field Coding, 2010, Proceedings of the IEEE Vehicular Technology Conference (VTC).

# Improved Error Protection for Uplink Control Signaling in 3GPP-LTE via Complex-Field Coding

Tumula V. K. Chaitanya[†], Erik G. Larsson[†], and Niclas Wiberg[‡]
[†]Dept. of Electrical Engineering (ISY), Linköping University, Linköping, Sweden. Email: {tvk,egl}@isy.liu.se
[‡]Ericsson Research, Linköping, Sweden. Email: niclas.wiberg@ericsson.com

***Abstract*—We study the uplink control signaling in 3GPP-Long Term Evolution (LTE) systems. Specifically, we propose a precoding method that uses complex-field coding (CFC) to improve the performance of the PUCCH format 2 control signaling. In the case of perfect channel state information (CSI) at the receiver and with a single receive antenna, the proposed method offers significant gains compared to the coding currently used in 3GPP-LTE. However the gains are marginal with two receive antennas. In order to examine the impact of channel estimation errors, we also derive the optimal detector for the case of imperfect receiver CSI, both for conventional coding and for the proposed CFC method.**

## I. Introduction

Fourth generation broadband wireless multiple access systems have data rate specifications in the order of hundreds of Mbit/sec (Mbps). For an LTE system with 20 MHz bandwidth (BW), the targets for downlink (DL) and uplink (UL) peak data rate requirements are 100 Mbps and 50 Mbps respectively [1]. LTE uses orthogonal frequency division multiple access (OFDMA) for transmission in the downlink. In the uplink, in order to avoid large peak-to-average ratios, and to facilitate the use of more power-efficient RF amplifiers, LTE uses single-carrier transmission based on DFT-spread OFDM (DFTS-OFDM). Sometimes this is also referred to as single-carrier frequency division multiple access (SC-FDMA) [2].

The LTE system has separate channels both in the downlink and the uplink to carry control channel information (CCI). For example, the base station (eNodeB in LTE terminology) schedules different customer premises equipments (CPEs) in a single downlink frame. This scheduling information has to be sent to each of the CPEs in a separate control channel to enable them to decode their data. In the uplink, the information about ACK/NACK for received downlink packets and also certain channel quality indicator (CQI) information have to be sent from each of the CPEs to the eNodeB. The error performance of CCI is an important factor to improve the overall system performance, especially for cell-edge users who experience large path losses and high inter-cell interference. In this paper, we focus on the uplink Layer 1/Layer 2 (L1/L2) control signaling in LTE.

The uplink L1/L2 control signaling in LTE uses two different methods to send the uplink control data, depending on whether or not the CPE has been assigned an uplink resource for uplink shared channel (UL-SCH) transmission:

- *Simultaneous transmission of UL-SCH*: In case the CPE has a valid scheduling grant, the uplink L1/L2 control signaling is time-multiplexed with the coded UL-SCH onto the so-called physical uplink shared channel (PUSCH) prior to DFTS-OFDM modulation.
- *No simultaneous transmission of UL-SCH*: In case the CPE does not have a valid scheduling grant, a separate physical channel, the physical uplink control channel (PUCCH) is used for the uplink L1/L2 control signaling. This method uses two different formats for sending the data:
  - *PUCCH format 1*: Scheduling requests and hybrid-automatic repeat request (H-ARQ) acknowledgments are sent using this format. This format can support a maximum of 2 bits of information per subframe.
  - *PUCCH format 2*: Usually periodic CQI information reports are sent using this format. Sometimes simultaneous transmission of H-ARQ acknowledgments and CQI reports is also done using this format. This format can support a maximum of 13 information bits per subframe.

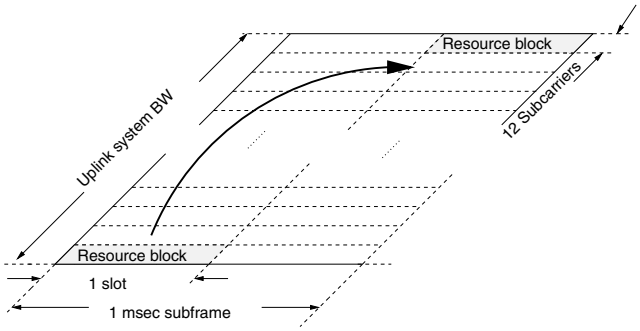


Figure 1. Uplink L1/L2 control signaling transmission on PUCCH (reproduced freely from [1, p. 398])

Fig. 1 shows the resources for uplink L1/L2 control signaling transmission on the PUCCH. These resources are located at the edges of the available bandwidth. Frequency hopping of these resources on the slot boundary provides frequency diversity to the control signaling. Each resource block consists of 12 OFDM subcarriers $\left(N_{\mathrm{sc}}^{\mathrm{RB}}\right)$ within each of two slots of an uplink subframe. The number of OFDM symbols in each slot

This work was supported in part by Ericsson, the Swedish Research Council (VR) and the Swedish Foundation for Strategic Research (SSF). E. G. Larsson is a Royal Swedish Academy of Sciences (KVA) Research Fellow supported by a grant from the Knut and Alice Wallenberg Foundation.

978-1-4244-2519-8/10/$26.00 ©2010 IEEE

Table I
RESOURCE BLOCK PARAMETERS FOR PUCCH FORMAT 2 TRANSMISSION

| Configuration | $N_{\mathrm{sc}}^{\mathrm{RB}}$ | $N_{\mathrm{symb}}^{\mathrm{RB}}$ | Data symbol indices | Reference signal symbols |
|---|---|---|---|---|
| Normal CP | 12 | 7 | 1,3,4,5,7 | 2,6 |
| Extended CP | 12 | 6 | 1,2,3,5,6 | 4 |

of a subframe $\left(N_{\mathrm{symb}}^{\mathrm{RB}}\right)$ depends on the cyclic prefix (CP) length, see Table I.

In this paper, we focus on the error protection for the CCI in the uplink of LTE. Specifically we are interested in the PUCCH format 2 control signaling which involves periodic reporting of CQI information separately or jointly with H-ARQ acknowledgments.[1] A $(20, N_I)$ Reed-Muller code is used for control signaling using the PUCCH format 2 [3], where $N_I$ is the number of information bits and $N_I \leq 13$.[2] Even though the control information is spread across two independent frequency bands (see Fig. 2), the specified code is not good at extracting the diversity mainly due to the short block length. To better extract this diversity and hence to improve the performance of the control signaling using the PUCCH format 2, we propose a method, where we precode pairs of modulated symbols selected from two independent frequency bands. We use a $2 \times 2$ complex-field coding (CFC) matrix [5], [6] for precoding and then transmit the precoded data on the channel. The simulation results in Section V show that the proposed transmission scheme offers significant gains on fading channels.

In practical systems like LTE, the receiver will only have imperfect CSI obtained from received pilots. The error in the channel estimate depends upon the number of pilots available and the channel estimation method used at the receiver. It is known that the optimal detectors designed for perfect CSI are not optimal for the receivers with imperfect CSI [8], [9]. In this paper, we derive the optimal detectors for the case of imperfect CSI for both the conventional and the proposed transmission methods. The simulation results in Section V show that the optimal detectors for the case of imperfect CSI can outperform the mismatched detector that inserts an estimated channel into the coherent decision metric.

## II. SYSTEM MODEL

CQI reports from the CPE to eNodeB are useful for channel-dependent scheduling in the downlink. A CQI report consists of a maximum of 11 information bits per subframe [3]. Since PUCCH format 1 can support at most two information bits per subframe, CQI information reports on PUCCH are sent using the PUCCH format 2. The structure of PUCCH format 2 depends on the CP configuration. Table I summarizes the configuration-dependent resource block parameters. Fig. 2 illustrates the PUCCH format 2 for the case of normal CP. The CQI information bits are coded using the $(20, N_I)$ Reed-Muller code generator matrix specified in [3], and the 20 coded output bits are modulated using quadrature phase shift keying (QPSK) constellation $(\mathcal{S})$.[3]

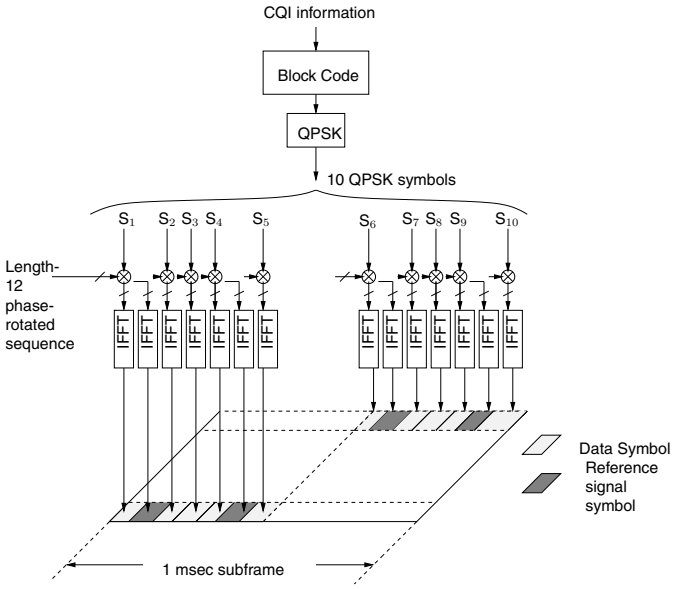


Figure 2. PUCCH format 2 for normal CP (reproduced freely from [1, p. 406])

Let $\mathbf{b}_I = [b_1, b_2, \cdots, b_{N_I}]^T$ be the vector of CCI information bits and let $\mathbf{G}$ denote the generator matrix of the Reed-Muller code. We write the coded output bit vector $\mathbf{b}_O = [b_1, b_2, \cdots, b_{20}]^T$ as $\mathbf{b}_O = \mathbf{G}\mathbf{b}_I$. Let $s_1, s_2, \cdots, s_{10}$ be the resulting QPSK symbols. The first five QPSK symbols $s_1, s_2, \cdots, s_5$ are transmitted in the first slot and the remaining five symbols $s_6, s_7, \cdots, s_{10}$ are transmitted in the last slot of a subframe. There are seven OFDM symbols in each slot. Two of them are used for reference signals to facilitate coherent demodulation. Each of the five QPSK data symbols is spread across the subcarriers in each symbol of the resource block by using a length-12 phase-rotated cell-specific sequence. Details about the phase-rotation sequence can be found in [4].

To simplify notation, we assume that the two resource blocks of a subframe which carry the control signaling information are adjacent in time and that the OFDM symbols which carry the QPSK symbols are contiguous (there is no reference signal symbols between them). Let $N_{\mathrm{symb}}^{\mathrm{data}}$ denote the number of data symbols in one subframe. For PUCCH format 2, $N_{\mathrm{symb}}^{\mathrm{data}} = 10$ (independently of the CP configuration).

At the receiver, after the fast Fourier transform (FFT) operation and after undoing the effect of the phase rotation sequence, the received signal on subcarrier $n$ of OFDM

[1]We are not considering PUCCH format 1 signaling as there is only one symbol (one BPSK or QPSK symbol depending on whether 1 or 2 bits of H-ARQ acknowledgments are to be sent) to be transmitted over a PUCCH resource. This single symbol is repeated over 10 DFTS-OFDM data symbols and 12 OFDM subcarriers per symbol, and hence it can extract the frequency diversity available across two resource blocks.

[2]In case of normal CP configuration, $N_I$ can only be $\leq 11$. However in case of extended CP configuration, there is a provision to code both CQI report bits and H-ARQ acknowledgment bits using the same Reed-Muller code. In this case $N_I \leq 13$.

[3]The LTE standard specifies a CPE specific scrambling sequence to scramble the coded bits before modulating [4]. However since the performance is independent of the scrambling sequence, we do not consider any scrambling sequence in this paper.

symbol $m$ is given by,

$$y_{mn} = h_{mn}s_m + w_{mn}, \quad 1 \le m \le N_{\text{symb}}^{\text{data}} \text{ and } 1 \le n \le N_{\text{sc}}^{\text{RB}} \tag{1}$$

In vector form, we write,

$$\mathbf{y}_m = \mathbf{h}_m s_m + \mathbf{w}_m, \quad 1 \le m \le N_{\text{symb}}^{\text{data}} \tag{2}$$

where

- $\mathbf{y}_m \triangleq \left[y_{m1}, y_{m2}, \cdots, y_{mN_{\text{sc}}^{\text{RB}}}\right]^T$ is the vector of received signals on all $N_{\text{sc}}^{\text{RB}}$ subcarriers of symbol $m$.
- $\mathbf{h}_m \triangleq \left[h_{m1}, h_{m2}, \cdots, h_{mN_{\text{sc}}^{\text{RB}}}\right]^T$ is the frequency domain channel vector of symbol $m$.
- $s_m$ is the $m$th transmitted QPSK symbol and
- $\mathbf{w}_m \triangleq \left[w_{m1}, w_{m2}, \cdots, w_{mN_{\text{sc}}^{\text{RB}}}\right]^T$ is the noise vector on OFDM symbol $m$, $\mathbf{w}_m \sim \mathcal{CN}(\mathbf{0}, N_0\mathbf{I})$.

Assuming that $\mathbf{h}_m$ is perfectly known to the receiver, the optimal detector for $s_m$, $1 \le m \le N_{\text{symb}}^{\text{data}}$, is obtained by maximizing the conditional probability $p(\mathbf{y}_m|\mathbf{h}_m, s_m)$. It can be shown that:

$$p(\mathbf{y}_m|\mathbf{h}_m, s_m) = \frac{1}{(\pi N_0)^{N_{\text{sc}}^{\text{RB}}}} \exp\left(-\frac{\|\mathbf{y}_m - \mathbf{h}_m s_m\|^2}{N_0}\right) \tag{3}$$

Maximizing the conditional probability in (3) is equivalent to:

$$\min_{s_m \in \mathcal{S}} \|\mathbf{y}_m - \mathbf{h}_m s_m\|^2 \Longleftrightarrow \min_{s_m \in \mathcal{S}} |s_m - \hat{s}_m|^2 \tag{4}$$

where

$$\hat{s}_m \triangleq \frac{\mathbf{h}_m^H \mathbf{y}_m}{\|\mathbf{h}_m\|^2} = s_m + \frac{\mathbf{h}_m^H \mathbf{w}_m}{\|\mathbf{h}_m\|^2} = s_m + \tilde{w}_m \tag{5}$$

and where $\tilde{w}_m \sim \mathcal{CN}\left(0, \frac{N_0}{\|\mathbf{h}_m\|^2}\right)$. Equation (5) corresponds to maximal-ratio-combining (MRC) at the receiver. Using the fact that $s_m \in \mathcal{S}$, assuming that all bits are a priori independent, and assuming equal a priori probabilities for the bits that constitute $s_m$, the a posteriori log-likelihood ratio (LLR) for the information bit that constitutes the in-phase component of $s_m$ can be written as:

$$\begin{aligned} L(b_I|\mathbf{y}_m) &= \log\left(\frac{\exp\left(-\frac{\|\mathbf{h}_m\|^2}{N_0}\left|\text{Re}\{\hat{s}_m\} - 1\right|^2\right)}{\exp\left(-\frac{\|\mathbf{h}_m\|^2}{N_0}\left|\text{Re}\{\hat{s}_m\} + 1\right|^2\right)}\right) \\ &= \frac{4\|\mathbf{h}_m\|^2}{N_0}\text{Re}\{\hat{s}_m\} \end{aligned} \tag{6}$$

From (6), we can see that the LLR of the bit $b_I$, constituting the in-phase component of $s_m$ is proportional to $\text{Re}\{\hat{s}_m\}$. Similarly we can show that the LLR for the quadrature-phase bit is proportional to $\text{Im}\{\hat{s}_m\}$:

$$L(b_Q|\mathbf{y}_m) = \frac{4\|\mathbf{h}_m\|^2}{N_0}\text{Im}\{\hat{s}_m\} \tag{7}$$

## III. Proposed Method for Control Signaling using Precoding

The Reed-Muller code with short block length used for control signaling is not able to extract all of the available frequency diversity. To extract more of this frequency diversity inherent in the resources for PUCCH format 2, we apply precoding on pairs of symbols from two independent slots of a subframe. More specifically, we transmit $x_m$ instead of $s_m$, where $x_m$ are obtained by a linear transformation of pairs of $s_m$ as follows:

$$\underbrace{\begin{bmatrix} x_m \\ x_{m+5} \end{bmatrix}}_{\triangleq \mathbf{x}} = \underbrace{\begin{bmatrix} \psi_{11} & \psi_{12} \\ \psi_{21} & \psi_{22} \end{bmatrix}}_{\triangleq \mathbf{\Psi}} \underbrace{\begin{bmatrix} s_m \\ s_{m+5} \end{bmatrix}}_{\triangleq \mathbf{s}}, \quad 1 \le m \le N_{\text{symb}}^{\text{data}}/2 \tag{8}$$

For precoding, we use a $2 \times 2$ CFC matrix $\mathbf{\Psi}$ generated using the designs specified in [5], [6]. It was shown that these designs provide full diversity (diversity of 2 in the present case). The key point is that the precoder improves the minimum product distance, which determines the performance in fading channels. We consider only unitary precoders, so that the performance on the AWGN channel is unaffected.[4] The transmit power also remains constant with the unitary precoder, because $\|\mathbf{s}\|^2 = \|\mathbf{\Psi}\mathbf{s}\|^2$. With the precoding, the received signal after undoing the effect of phase rotation sequence on subcarrier $n$ of OFDM symbols $m$ and $(m+5)$ can be written as in (9), shown on top of the next page.

Using the definitions from Section II, let $\mathbf{y}_m$, $\mathbf{h}_m$ and $\mathbf{w}_m$ denote the vectors of received signals, frequency domain channel gains and noise vector respectively, for OFDM symbol $m$. Similarly, let the corresponding vectors for symbol $(m+5)$ be $\mathbf{y}_{(m+5)}$, $\mathbf{h}_{(m+5)}$ and $\mathbf{w}_{(m+5)}$.

We write the combined received signal vector for all the subcarriers in OFDM symbols $m$ and $(m+5)$ as in (10) shown at the top of the next page.

In (10), $\mathbf{y}$ is a $2N_{\text{sc}}^{\text{RB}} \times 1$ received signal vector, $\mathbf{F}$ is a $2N_{\text{sc}}^{\text{RB}} \times 2$ tall channel matrix with columns $\mathbf{f}_1, \mathbf{f}_2$ and $\mathbf{w}$ is a $2N_{\text{sc}}^{\text{RB}} \times 1$ noise vector. The optimal detector for $\mathbf{s}$ is obtained by maximizing the conditional distribution of $\mathbf{y}|\mathbf{F}, \mathbf{\Psi}, \mathbf{s}$, which is given by:

$$p(\mathbf{y}|\mathbf{F}, \mathbf{\Psi}, \mathbf{s}) = \frac{1}{(\pi N_0)^{2N_{\text{sc}}^{\text{RB}}}} \exp\left(-\frac{\|\mathbf{y} - \mathbf{F}\mathbf{\Psi}\mathbf{s}\|^2}{N_0}\right) \tag{11}$$

Maximizing (11) is the same as:

$$\min_{\mathbf{s} \in \mathcal{S}^2} \|\mathbf{y} - \mathbf{F}\mathbf{\Psi}\mathbf{s}\|^2 \tag{12}$$

Let the QR decomposition of $\mathbf{F}$ be given by $\mathbf{F} = \mathbf{Q}\mathbf{R}$, where $\mathbf{Q}$ is a $2N_{\text{sc}}^{\text{RB}} \times 2$ semi-unitary matrix ($\mathbf{Q}^H\mathbf{Q} = \mathbf{I}$) and $\mathbf{R}$ is a $2 \times 2$ upper triangular matrix. Owing to the structure of $\mathbf{F}$, it turns out that

$$\mathbf{Q} = \left[\frac{\mathbf{f_1}}{\|\mathbf{f_1}\|}, \frac{\mathbf{f_2}}{\|\mathbf{f_2}\|}\right] \tag{13}$$

[4]Note that if $\mathbf{\Psi}^H\mathbf{\Psi} = \mathbf{I}$, then $\left\|\mathbf{\Psi}\left(\mathbf{s} - \mathbf{s}'\right)\right\| = \left\|\mathbf{s} - \mathbf{s}'\right\|$ $\forall \mathbf{s}, \mathbf{s}' \in \mathcal{S}^2$.

$$\begin{aligned}\begin{bmatrix} y_{mn} \\ y_{(m+5)n} \end{bmatrix} &= \begin{bmatrix} h_{mn} & 0 \\ 0 & h_{(m+5)n} \end{bmatrix} \begin{bmatrix} \psi_{11} & \psi_{12} \\ \psi_{21} & \psi_{22} \end{bmatrix} \begin{bmatrix} s_m \\ s_{m+5} \end{bmatrix} + \begin{bmatrix} w_{mn} \\ w_{(m+5)n} \end{bmatrix} \\ &= \begin{bmatrix} h_{mn} & 0 \\ 0 & h_{(m+5)n} \end{bmatrix} \begin{bmatrix} x_m \\ x_{m+5} \end{bmatrix} + \begin{bmatrix} w_{mn} \\ w_{(m+5)n} \end{bmatrix} \end{aligned} \tag{9}$$

$$\underbrace{\begin{bmatrix} y_{m1} \\ \vdots \\ y_{mN_{\mathrm{sc}}^{\mathrm{RB}}} \\ y_{(m+5)1} \\ \vdots \\ y_{(m+5)N_{\mathrm{sc}}^{\mathrm{RB}}} \end{bmatrix}}_{\triangleq \mathbf{y}} = \underbrace{\begin{bmatrix} h_{m1} & 0 \\ \vdots & \vdots \\ h_{mN_{\mathrm{sc}}^{\mathrm{RB}}} & 0 \\ 0 & h_{(m+5)1} \\ \vdots & \vdots \\ 0 & h_{(m+5)N_{\mathrm{sc}}^{\mathrm{RB}}} \end{bmatrix}}_{\triangleq \mathbf{F} \triangleq [\mathbf{f}_1, \mathbf{f}_2]} \underbrace{\begin{bmatrix} \psi_{11} & \psi_{12} \\ \psi_{21} & \psi_{22} \end{bmatrix}}_{\mathbf{\Psi}} \underbrace{\begin{bmatrix} s_m \\ s_{m+5} \end{bmatrix}}_{\mathbf{s}} + \underbrace{\begin{bmatrix} w_{m1} \\ \vdots \\ w_{mN_{\mathrm{sc}}^{\mathrm{RB}}} \\ w_{(m+5)1} \\ \vdots \\ w_{(m+5)N_{\mathrm{sc}}^{\mathrm{RB}}} \end{bmatrix}}_{\triangleq \mathbf{w}} \tag{10}$$

and

$$\mathbf{R} = \mathrm{diag}(\|\mathbf{f}_1\|, \|\mathbf{f}_2\|) = \mathrm{diag}(\|\mathbf{h}_m\|, \|\mathbf{h}_{(m+5)}\|) \tag{14}$$

Following [7], we have

$$\begin{aligned}\|\mathbf{y} - \mathbf{F\Psi s}\|^2 &= \left\|\mathbf{QQ}^H (\mathbf{y} - \mathbf{F\Psi s})\right\|^2 \\ &\quad + \left\|\left(\mathbf{I} - \mathbf{QQ}^H\right)(\mathbf{y} - \mathbf{F\Psi s})\right\|^2 \\ &= \left\|\mathbf{Q}^H\mathbf{y} - \mathbf{R\Psi s}\right\|^2 + \left\|\left(\mathbf{I} - \mathbf{QQ}^H\right)\mathbf{y}\right\|^2\end{aligned}$$

The term $\left\|\left(\mathbf{I} - \mathbf{QQ}^H\right)\mathbf{y}\right\|^2$ is independent of $\mathbf{s}$, so (12) is equivalent to

$$\min_{\mathbf{s}\in\mathcal{S}^2} \left\|\mathbf{Q}^H\mathbf{y} - \mathbf{R\Psi s}\right\|^2 \tag{15}$$

Pre-multiplying (10) with $\mathbf{Q}^H$, we get

$$\mathbf{Q}^H\mathbf{y} \triangleq \underbrace{\begin{bmatrix} \bar{y}_m \\ \bar{y}_{m+5} \end{bmatrix}}_{\triangleq \mathbf{y}_{\mathrm{equ}}} = \underbrace{\begin{bmatrix} \|\mathbf{h}_m\| & 0 \\ 0 & \|\mathbf{h}_{(m+5)}\| \end{bmatrix}}_{\mathbf{R}} \begin{bmatrix} \psi_{11} & \psi_{12} \\ \psi_{21} & \psi_{22} \end{bmatrix} \begin{bmatrix} s_m \\ s_{m+5} \end{bmatrix} + \begin{bmatrix} \bar{w}_m \\ \bar{w}_{(m+5)} \end{bmatrix} \tag{16}$$

where $\bar{w}_m$ and $\bar{w}_{(m+5)}$ are i.i.d. $\mathcal{CN}(0, N_0)$ since $\mathbf{Q}$ is semi-unitary. Using the structure of $\mathbf{f}_1$ and $\mathbf{f}_2$, we can show that

$$\begin{bmatrix} \bar{y}_m \\ \bar{y}_{(m+5)} \end{bmatrix} = \begin{bmatrix} \frac{\mathbf{h}_m^H \mathbf{y}_m}{\|\mathbf{h}_m\|} \\ \frac{\mathbf{h}_{(m+5)}^H \mathbf{y}_{(m+5)}}{\|\mathbf{h}_{(m+5)}\|} \end{bmatrix}$$

and

$$\begin{bmatrix} \bar{w}_m \\ \bar{w}_{(m+5)} \end{bmatrix} = \begin{bmatrix} \frac{\mathbf{h}_m^H \mathbf{w}_m}{\|\mathbf{h}_m\|} \\ \frac{\mathbf{h}_{(m+5)}^H \mathbf{w}_{(m+5)}}{\|\mathbf{h}_{(m+5)}\|} \end{bmatrix}$$

The interpretation is that we can apply MRC independently on all the subcarriers of symbols $m$ and $(m+5)$, and then perform joint detection with the system matrix $\mathbf{R\Psi}$. From (11), (15) and (16), we can write

$$p(\mathbf{y}|\mathbf{F}, \mathbf{\Psi}, \mathbf{s}) \propto \frac{1}{(\pi N_0)^{2N_{\mathrm{sc}}^{\mathrm{RB}}}} \exp\left(-\frac{\|\mathbf{y}_{\mathrm{equ}} - \mathbf{R\Psi s}\|^2}{N_0}\right) \tag{17}$$

To compute the posterior LLR for the information bits that constitute $s_k$, we use:

$$L(b_{k,i}|\mathbf{y}) = \log\left(\frac{\sum_{\mathbf{s}:b_{k,i}(\mathbf{s})=1} \exp\left(-\frac{\|\mathbf{y}_{\mathrm{equ}} - \mathbf{R\Psi s}\|^2}{N_0}\right)}{\sum_{\mathbf{s}:b_{k,i}(\mathbf{s})=0} \exp\left(-\frac{\|\mathbf{y}_{\mathrm{equ}} - \mathbf{R\Psi s}\|^2}{N_0}\right)}\right) \tag{18}$$

where $\mathbf{s} : b_{k,i}(\mathbf{s}) = \beta$ means all $\mathbf{s}$ for which the $i$th bit of $s_k$ is equal to $\beta$. Note that here we are demodulating two symbols at a time, and each LLR computation involves the evaluation of 16 terms in (18). This is somewhat more complex than the conventional detection in Section II.

## IV. Optimal Detectors with Imperfect Channel State Information (CSI)

In this section, we derive the optimal detectors when the receiver has imperfect CSI. Let the estimated channel on all $N_{\mathrm{sc}}^{\mathrm{RB}}$ subcarriers of the $m$th OFDM symbol be denoted by $\hat{\mathbf{h}}_m \triangleq \left[\hat{h}_{m1}, \hat{h}_{m2}, \cdots, \hat{h}_{mN_{\mathrm{sc}}^{\mathrm{RB}}}\right]^T$. The detectors obtained by replacing $\mathbf{h}_m$ with $\hat{\mathbf{h}}_m$ in (4) and (15) will be referred to as mismatched detectors, and are not optimal for a receiver with imperfect CSI [8], [9].

### A. Conventional Coding Case

Consider the system model as in (2), and suppose that $\mathbf{h}_m \sim \mathcal{CN}(\mathbf{0}, \mathbf{R}_{hh})$, where $\mathbf{R}_{hh}$ is the covariance matrix of the channel gains on all $N_{\mathrm{sc}}^{\mathrm{RB}}$ subcarriers, i.e.,

$$\mathbf{R}_{hh} = E\left(\mathbf{h}_m \mathbf{h}_m^H\right), \quad 1 \le m \le N_{\mathrm{symb}}^{\mathrm{data}} \tag{19}$$

We assume that the imperfect CSI at the receiver can be modeled as

$$\hat{\mathbf{h}}_m = \mathbf{h}_m + \boldsymbol{\delta}_m \tag{20}$$

where $\boldsymbol{\delta}_m$ denotes the error in the estimate of the channel and $\boldsymbol{\delta}_m \sim \mathcal{CN}(\mathbf{0}, \mathbf{R}_{\delta\delta})$, i.e., we assume that the distribution of $\boldsymbol{\delta}_m$ is same for all symbols. The structure of $\mathbf{R}_{\delta\delta}$ depends on the channel estimation method used for estimating the channel. We also assume that $\boldsymbol{\delta}_m$ is independent of $\mathbf{h}_m$ and $\mathbf{w}_m$. Under these assumptions, we can write $\hat{\mathbf{h}}_m \sim \mathcal{CN}(\mathbf{0}, \mathbf{R}_{hh} + \mathbf{R}_{\delta\delta})$.

We now derive the optimal detector under imperfect CSI case by computing the conditional probability

$p\left(\mathbf{y}_m|\hat{\mathbf{h}}_m, s_m\right)$. We note that $\mathbf{y}_m, \hat{\mathbf{h}}_m$ are jointly Gaussian, conditioned on $s_m$, with the following joint distribution:

$$\begin{bmatrix} \mathbf{y}_m \\ \hat{\mathbf{h}}_m \end{bmatrix} \sim \mathcal{CN}\left(\mathbf{0}, \begin{bmatrix} N_0\mathbf{I} + |s_m|^2 \mathbf{R}_{hh} & \mathbf{R}_{hh} s_m \\ \mathbf{R}_{hh} s_m^* & \mathbf{R}_{hh} + \mathbf{R}_{\delta\delta} \end{bmatrix}\right) \tag{21}$$

We can now write the following conditional distribution:

$$\mathbf{y}_m|\hat{\mathbf{h}}_m, s_m \sim \mathcal{CN}\left(\bar{\mathbf{y}}_m, \mathbf{P}\right) \tag{22}$$

where [11]

$$\bar{\mathbf{y}}_m \triangleq \left[\mathbf{R}_{hh}\left(\mathbf{R}_{hh} + \mathbf{R}_{\delta\delta}\right)^{-1}\right] \hat{\mathbf{h}}_m s_m \tag{23}$$

and

$$\mathbf{P} \triangleq \left(N_0\mathbf{I} + |s_m|^2 \mathbf{R}_{hh}\left(\mathbf{I} - \left(\mathbf{R}_{hh} + \mathbf{R}_{\delta\delta}\right)^{-1}\mathbf{R}_{hh}\right)\right) \tag{24}$$

Hence we can write

$$\begin{aligned} p\left(\mathbf{y}_m|\hat{\mathbf{h}}_m, s_m\right) &= \frac{1}{\pi^{N_{\text{sc}}^{\text{RB}}} \det\left(\mathbf{P}\right)} \exp\Big(-\left(\mathbf{y}_m - \bar{\mathbf{y}}_m\right)^H \\ &\quad \mathbf{P}^{-1}\left(\mathbf{y}_m - \bar{\mathbf{y}}_m\right)\Big) \end{aligned} \tag{25}$$

The analysis done in this subsection is valid for any diversity combining system with imperfect CSI. Note that for the conditional distribution in (25) to be a valid, we need the sum $\mathbf{R}_{hh} + \mathbf{R}_{\delta\delta}$ to be invertible, so that (23) and (24) exist. For PUCCH format 2, the MRC is done on successive subcarriers which have correlated channel gains. Hence $\mathbf{R}_{hh}$ is not necessarily invertible.

For $\mathbf{R}_{\delta\delta}$ we consider two different models:

$$\mathbf{R}_{\delta\delta} = \rho N_0 \mathbf{I}, \quad \rho > 0 \tag{26}$$

$$\text{and} \quad \mathbf{R}_{\delta\delta} = \sigma N_0 \mathbf{u}\mathbf{u}^H + \frac{\sigma N_0}{C}\mathbf{I}, \quad \sigma > 0 \text{ and } C > 0 \tag{27}$$

where $\mathbf{u} \triangleq [1, 1, \ldots, 1]^T$. We considered these two models for $\mathbf{R}_{\delta\delta}$ as they represent the two extreme cases of possible estimation errors in practice. The model (26) reflects the special case where the estimation error is independent across all the subcarriers of a resource block in each OFDM symbol. The model in (27) corresponds to the case that the estimation error across the subcarriers is practically the same. Estimators in practice would yield a $\mathbf{R}_{\delta\delta}$ with a structure somewhere in between of (26) and (27), probably closer to (27) than to (26). In our numerical results, we will include both models.

Under the assumptions of (26) or (27), $\mathbf{P}^{-1}$ is Hermitian and positive definite. We can write $\mathbf{P}^{-1} = \mathbf{P}^{-1/2}\mathbf{P}^{-1/2}$, where $\mathbf{P}^{-1/2}$ is a positive definite square-root of $\mathbf{P}^{-1}$. Hence we can rewrite (25) as

$$p\left(\mathbf{y}_m|\hat{\mathbf{h}}_m, s_m\right) = \frac{1}{\pi^{N_{\text{sc}}^{\text{RB}}} \det\left(\mathbf{P}\right)} \exp\left(-\left\|\tilde{\mathbf{y}}_m - \check{\mathbf{y}}_m\right\|^2\right) \tag{28}$$

where

$$\tilde{\mathbf{y}}_m \triangleq \mathbf{P}^{-1/2}\mathbf{y}_m,$$

$$\check{\mathbf{y}}_m \triangleq \mathbf{P}^{-1/2}\bar{\mathbf{y}}_m = \mathbf{P}^{-1/2}\left[\mathbf{R}_{hh}\left(\mathbf{R}_{hh} + \mathbf{R}_{\delta\delta}\right)^{-1}\right] \hat{\mathbf{h}}_m s_m$$

Using (28), for the imperfect CSI case, we can write the LLR's for the bits that constitute $s_m$ as:

$$L\left(b_i|\mathbf{y}_m\right) = \log\left(\frac{\sum_{s_m: b_i(s_m)=1} \exp\left(-\left\|\tilde{\mathbf{y}}_m - \check{\mathbf{y}}_m\right\|^2\right)}{\sum_{s_m: b_i(s_m)=0} \exp\left(-\left\|\tilde{\mathbf{y}}_m - \check{\mathbf{y}}_m\right\|^2\right)}\right) \tag{29}$$

### *B. Proposed Precoding Case*

The combined received signal vector in (10) can equivalently be written as

$$\mathbf{y} = \mathbf{X}\mathbf{f} + \mathbf{w} \tag{30}$$

where $\mathbf{X} = \text{diag}\left(x_m\mathbf{I}, x_{m+5}\mathbf{I}\right)$ and $\mathbf{f} = \begin{bmatrix} \mathbf{h}_m^T & \mathbf{h}_{m+5}^T \end{bmatrix}^T$. Assume that the estimate of $\mathbf{f}$ can be written as $\hat{\mathbf{f}} = \mathbf{f} + \boldsymbol{\delta}$, where $\boldsymbol{\delta} = \begin{bmatrix} \boldsymbol{\delta}_m^T & \boldsymbol{\delta}_{m+5}^T \end{bmatrix}^T$ is the corresponding estimation error with $\boldsymbol{\delta}_m$ and $\boldsymbol{\delta}_{m+5}$ being independent. Then $\mathbf{y}$ and $\hat{\mathbf{f}}$ are jointly Gaussian conditioned on $\mathbf{x}$, and the joint conditional distribution is given by:

$$\begin{bmatrix} \mathbf{y} \\ \hat{\mathbf{f}} \end{bmatrix} \sim \mathcal{CN}\left(\mathbf{0}, \begin{bmatrix} \mathbf{A} & \mathbf{B} \\ \mathbf{B}^H & \mathbf{D} \end{bmatrix}\right) \tag{31}$$

where

$$\begin{aligned} \mathbf{A} &= \text{diag}\left(|x_m|^2 \mathbf{R}_{hh} + N_0\mathbf{I}, |x_{m+5}|^2 \mathbf{R}_{hh} + N_0\mathbf{I}\right) \\ \mathbf{B} &= \text{diag}\left(x_m\mathbf{R}_{hh}, x_{m+5}\mathbf{R}_{hh}\right) \\ \mathbf{D} &= \text{diag}\left(\mathbf{R}_{hh} + \mathbf{R}_{\delta\delta}, \mathbf{R}_{hh} + \mathbf{R}_{\delta\delta}\right) \end{aligned}$$

Using (31), we can write the conditional distribution of $\mathbf{y}|\hat{\mathbf{f}}, \boldsymbol{\Psi}, \mathbf{s}$ as

$$\begin{aligned} p\left(\mathbf{y}|\hat{\mathbf{f}}, \boldsymbol{\Psi}, \mathbf{s}\right) &= \frac{1}{\pi^{2N_{\text{sc}}^{\text{RB}}} \det\left(\mathbf{T}\right)} \exp\Big(-\left(\mathbf{y} - \bar{\mathbf{y}}\right)^H \\ &\quad \mathbf{T}^{-1}\left(\mathbf{y} - \bar{\mathbf{y}}\right)\Big) \end{aligned} \tag{32}$$

where

$$\bar{\mathbf{y}} \triangleq \mathbf{M}\mathbf{D}^{-1}\hat{\mathbf{F}}\boldsymbol{\Psi}\mathbf{s} \tag{33}$$

and where $\mathbf{M} = \text{diag}\left(\mathbf{R}_{hh}, \mathbf{R}_{hh}\right)$, $\hat{\mathbf{F}}$ is defined similarly to $\mathbf{F}$ in (10) with $h_{mn}$ replaced by $\hat{h}_{mn}$ and $\mathbf{T} \triangleq \text{diag}\left(\mathbf{P}_m, \mathbf{P}_{m+5}\right)$ with

$$\mathbf{P}_m \triangleq N_0\mathbf{I} + |x_m|^2 \mathbf{R}_{hh}\left(\mathbf{I} - \left(\mathbf{R}_{hh} + \mathbf{R}_{\delta\delta}\right)^{-1}\mathbf{R}_{hh}\right),$$

$$\mathbf{P}_{m+5} \triangleq N_0\mathbf{I} + |x_{m+5}|^2 \mathbf{R}_{hh}\left(\mathbf{I} - \left(\mathbf{R}_{hh} + \mathbf{R}_{\delta\delta}\right)^{-1}\mathbf{R}_{hh}\right)$$

With the assumption in (26) or (27), the sum $\mathbf{R}_{hh} + \mathbf{R}_{\delta\delta}$ is invertible and hence the conditional distribution in (32) can be written as:

$$p\left(\mathbf{y}|\hat{\mathbf{f}}, \boldsymbol{\Psi}, \mathbf{s}\right) = \frac{1}{\pi^{2N_{\text{sc}}^{\text{RB}}} \det\left(\mathbf{T}\right)} \exp\left(-\left\|\tilde{\mathbf{y}} - \check{\mathbf{y}}\right\|^2\right) \tag{34}$$

where

$$\tilde{\mathbf{y}} \triangleq \mathbf{T}^{-1/2}\mathbf{y},$$

$$\check{\mathbf{y}} \triangleq \mathbf{T}^{-1/2}\bar{\mathbf{y}} = \mathbf{T}^{-1/2}\mathbf{M}\mathbf{D}^{-1}\hat{\mathbf{F}}\boldsymbol{\Psi}\mathbf{s}$$

Using (34), in case of the proposed method with imperfect CSI, we can write the posterior LLRs for the information bits as:

$$L\left(b_{k,i}|\mathbf{y}\right) = \log\left(\frac{\sum_{\mathbf{s}:b_{k,i}(\mathbf{s})=1}\exp\left(-\left\|\tilde{\mathbf{y}}-\check{\mathbf{y}}\right\|^2\right)}{\sum_{\mathbf{s}:b_{k,i}(\mathbf{s})=0}\exp\left(-\left\|\tilde{\mathbf{y}}-\check{\mathbf{y}}\right\|^2\right)}\right) \quad (35)$$

## V. Simulation Results

In this section, we present simulation results to illustrate the performance of the proposed precoding approach for the cases of perfect CSI (P-CSI) and imperfect CSI (I-CSI) with different detectors. Monte-Carlo simulation was used to obtain the block-error rate (BLER) performance, and at each point in the curves, we observed at least 1000 block errors. We considered an OFDM system with 300 subcarriers and a carrier spacing of 15 kHz. For the Rayleigh fading process, we used the ITU - Vehicular A channel model with 20 Hz Doppler frequency. We used normal CP configuration for $N_I = 11$ and extended CP configuration for $N_I = 13$. Channels were generated assuming the reference signals between the data symbols as shown in Fig. 2. We used a pseudo-random bit interleaver and de-interleaver pair, independently chosen for each Monte-Carlo run. For the proposed method with precoding as in (8), we used

$$\mathbf{\Psi} = \begin{bmatrix} \frac{1}{\sqrt{2}} & \frac{1}{2} - j\frac{1}{2} \\ \frac{1}{\sqrt{2}} & -\frac{1}{2} + j\frac{1}{2} \end{bmatrix}.$$

### A. Results with Perfect Channel State Information (P-CSI) at the Receiver

First we show the Reed-Muller code performance with hard-decision and soft-decision decoding. Fig. 3 shows the performance comparison for the conventional coding and for the proposed method both with hard-decision and soft-decision decoding. We see that the proposed method is performing better than the conventional coding method for both hard-decision and soft-decision decoding. With P-CSI at the receiver and for $N_I = 13$, at a BLER of $10^{-2}$, the proposed method has a performance gain up to 2.5 dB and 4 dB over the conventional coding method with soft-decision decoding and hard-decision decoding, respectively. The gain for the proposed method comes from the complex-field spreading of the information over the two independent frequency slots.

### B. Results with Imperfect Channel State Information (I-CSI) at the Receiver

Next, we illustrate the performance when the receiver only has an estimate of the channel, for various cases of CSI and detector combinations. We consider the coherent detector for P-CSI, the optimum detector for I-CSI, and the mismatch detector for I-CSI, obtained by inserting a channel estimate into the P-CSI decision metric. Table II summarizes the detectors considered. As the reference signal occupies all $N_{\text{sc}}^{\text{RB}}$ subcarriers, on an AWGN channel, averaging the received signal on a reference symbol results in an estimation error variance equal to $\frac{N_0}{N_{\text{sc}}^{\text{RB}}}$. So for the simulations, we took $\rho = \frac{1}{N_{\text{sc}}^{\text{RB}}}$, $C = 10$ and $\sigma$ is chosen such that the $\text{trace}(\mathbf{R}_{\delta\delta})$ is same for both forms of estimation error in (26) and (27).

Table II
Summary of various CSI and detector combinations

| Method | Channel, LLR equation number for the conventional method | Channel, LLR equation number for the proposed method |
|---|---|---|
| P-CSI with optimal detector | $\mathbf{h}_m$, (6) and (7) | $\mathbf{F}$, (18) |
| I-CSI with mismatched detector | $\hat{\mathbf{h}}_m$, (6) and (7) | $\hat{\mathbf{F}}$, (18) |
| I-CSI with optimal detector | $\hat{\mathbf{h}}_m$, (29) | $\hat{\mathbf{F}}$, (35) |

The choice of $C$ is somewhat arbitrary, and was taken to yield a $\mathbf{R}_{\delta\delta}$ matrix with condition number about 120.

Fig. 4 illustrates the performance comparison for different cases of CSI knowledge at the receiver. From Fig. 4(a), we see that with $\mathbf{R}_{\delta\delta}$ of the form (26) and using the mismatched detector with I-CSI at the receiver yields a performance degradation of 3 dB and 2 dB compared to the case of P-CSI for the conventional coding and the proposed precoding method, respectively. However with I-CSI at the receiver, when we use the optimum detectors derived in Section IV, the losses reduce to 1 dB and 0.5 dB respectively. The reason for this gain with the optimal detector for the I-CSI case over the mismatched detector is as follows. Since with the simulation parameters used here, the channel is nearly flat across the subcarriers in each OFDM symbol of the PUCCH resource. Therefore, the optimal detector can perform better by averaging out the estimation error as it know that $\mathbf{R}_{\delta\delta} \propto \mathbf{I}$. When $\mathbf{R}_{\delta\delta}$ has the structure of (27), as shown in Fig. 4(b), using the optimal detector for I-CSI case does not provide any gain over the mismatched detector. In this case, the estimation error is nearly the same across all the subcarriers of each OFDM symbol and hence the optimal detector cannot average out the estimation error.

### C. Result with Two Receive Antennas

Fig. 5 shows performance results for the case of 2 receive antennas. From the plot, we can observe that the performance gap between the proposed method and the conventional coding method is reduced for all the cases of CSI and detector combinations.

## VI. Conclusions

We have proposed improvements to the PUCCH format 2 control signaling in the uplink of an LTE system. The proposed method extracts the frequency diversity inherent in the channel by using the complex field code designs of [5], [6]. Simulation results show that significant gains can be achieved with a single receive antenna, but that the gains become marginal with two receiving antennas. We also derived optimal detectors for the conventional coding and the proposed precoding methods, when the receiver has imperfect CSI.

## References

[1] E. Dahlman, S. Parkvall, J. Sköld, and P. Beming, *3G Evolution- HSPA and LTE for Mobile Broadband,* 2nd ed., Academic Press, 2008.

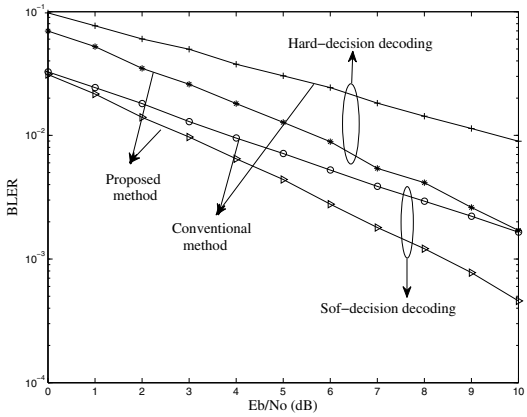


(a) (20,11) - Reed-Muller code

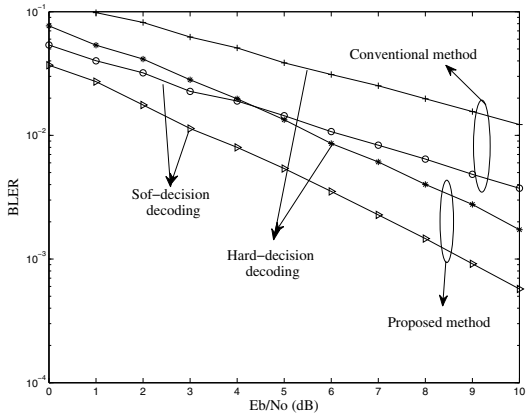


(b) (20,13) - Reed-Muller code

Figure 3. Performance of control signaling using PUCCH format 2 with $(20, N_I)$ Reed-Muller code, for $N_I = 11$ and 13. We assumed single transmit and single receive antenna with P-CSI at the receiver for these simulations. For soft decoding of Reed-Muller code, we used an algorithm based on Hadamard matrices as described in [10].

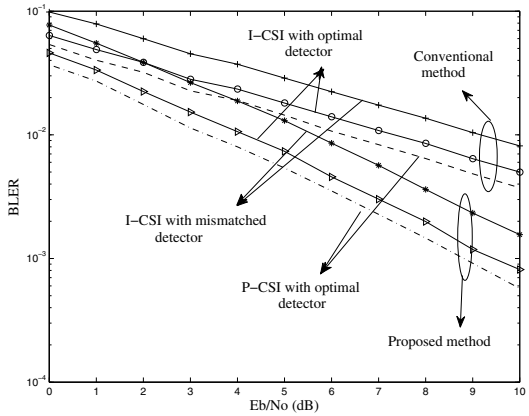


(a) With estimation error of form (26)

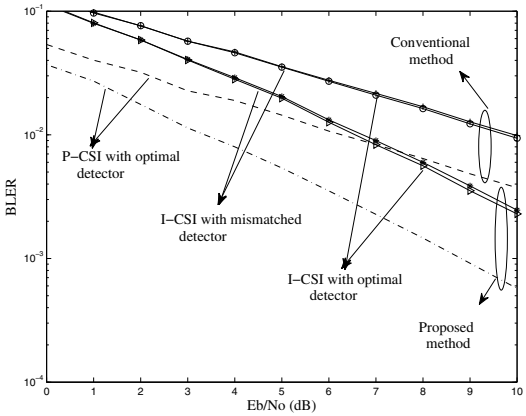


(b) With estimation error of form (27)

Figure 4. Comparison of performance for various cases summarized in Table II. We used (20,13) Reed-Muller code with soft-decision decoding.

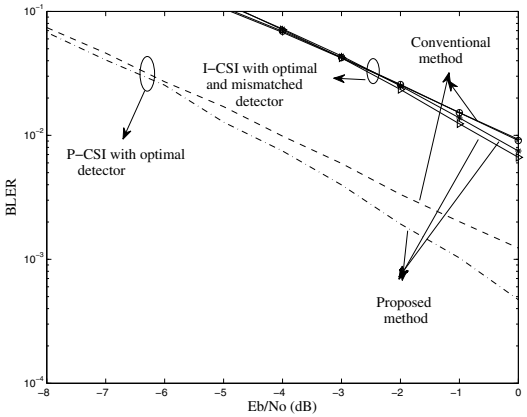


Figure 5. Performance comparison of the proposed method and the conventional coding method for the case when the receiver has two antennas. Here we used (20,13) Reed-Muller code with soft-decision decoding. The estimation error $\boldsymbol{\delta}_m$ is assumed to be of the form (27). We applied MRC for the signals received on two receive branches.


[2] D. Astély et al., "LTE: The evolution of mobile broadband," *IEEE Comm. Magazine,* vol. 47, pp. 44-51, April 2009.

[3] 3GPP TS 36.212, Multiplexing and Channel Coding for Evolved - UTRA, v.8.6.0., March 2009.

[4] 3GPP TS 36.211, Physical Channels and Modulation for Evolved - UTRA, v.8.6.0., March 2009.

[5] J. Boutros and E. Viterbo, "Signal space diversity, a power- and bandwidth-efficient diversity technique for the Rayleigh fading channel," *IEEE Trans. Inform. Theory*, vol. 44, pp. 1453-1467, July 1998.

[6] Z. Li, Y. Xin, and G. B. Giannakis, "Linear constellation precoding for OFDM with maximum multipath diversity and coding gains," *IEEE Trans. Comm.*, vol. 51, pp. 416-427, March 2003.

[7] E. G. Larsson, "MIMO detection methods: How they work," *IEEE Sig. Proc. Magazine*, vol. 26, pp. 91-95, May 2009.

[8] G. Taricco and E. Bigleri, "Space-time decoding with imperfect channel estimation," *IEEE Trans Wireless Commun.*, vol. 4, pp. 1874-1888, July 2005.

[9] E. G. Larsson and J. Jaldén, "Soft MIMO detection at fixed complexity via partial marginalization," *IEEE Trans. Signal. Proc.*, vol. 56, pp. 3397-3407, Aug. 2008.

[10] Y. Be'ery and J. Snyders, "Optimal soft decision block decoders based on fast Hadamard transform," *IEEE Trans. Inform. Theory*, vol. 32, pp. 355–364, May 1986.

[11] T. Söderström, *Discrete-time Stochastic Systems - Estimation and Control*, second edition, Springer-Verlag, London, UK, 2002.